



Calcium binding to *Procambarus clarkii* sarcoplasmic calcium binding protein splice variants

Suzanne E. Rohrback^a, Michele G. Wheatly^b, Christopher M. Gillen^{a,*}

^a Department of Biology, Kenyon College, Gambier, OH 43022, United States

^b Department of Biological Sciences, Wright State University, Dayton, OH 45435, United States

ARTICLE INFO

Article history:

Received 2 July 2014

Received in revised form 22 September 2014

Accepted 23 September 2014

Available online 28 September 2014

Keywords:

Affinity

Crayfish

EF hand

Fluorescence

Muscle

ABSTRACT

Sarcoplasmic calcium binding protein (SCP) is a high-affinity calcium buffering protein expressed in muscle of crayfish and other invertebrates. In previous work, we identified three splice variants of *Procambarus clarkii* SCP (pcSCP1a, pcSCP1b, and pcSCP1c) that differ in a 37 amino acid region that lies mainly between the 2nd and 3rd EF-hand calcium binding domain. To evaluate the function of the proteins encoded by the pcSCP1 transcripts, we produced recombinant pcSCP1 and used tryptophan fluorescence to characterize calcium binding. Tryptophan fluorescence of pcSCP1a decreased in response to increased calcium, while tryptophan fluorescence of the pcSCP1b and pcSCP1c variants increased. We estimated calcium binding constants and Hill coefficients with two different equations: the standard Hill equation and a modified Hill equation that accounts for contributions from two different tryptophans. The approaches gave similar results. Steady-state calcium binding constants (K_d) ranged from $2.7 \pm 0.7 \times 10^{-8}$ M to $5.6 \pm 0.1 \times 10^{-7}$ M, consistent with previous work. Variants displayed significantly different apparent calcium affinities, which were decreased in the presence of magnesium. Calcium K_d was lowest for pcSCP1a and highest for pcSCP1c. Site-directed mutagenesis of pcSCP1c residues to the amino acids of pcSCP1b decreased the calcium K_d , identifying residues outside the EF-hand domains that contribute to calcium binding in crayfish SCP.

© 2014 Elsevier Inc. All rights reserved.

1. Introduction

Sarcoplasmic calcium binding protein (SCP) is an invertebrate EF-hand calcium binding protein (Hermann and Cox, 1995).¹ Similar to vertebrate parvalbumin, SCP binds calcium with high affinity (binding constants $\sim 10^{-7}$ to 10^{-8} M) and is highly expressed in fast-twitch muscle (Cox et al., 1976; Wnuk et al., 1979; Heizmann et al., 1982; Wnuk and Jauregui-Adell, 1983; Leberer and Pette, 1986a,b). However, the calcium binding properties of SCP differ from those of vertebrate parvalbumin. Each ~ 12 kDa parvalbumin molecule contains two high-affinity calcium binding sites that bind magnesium with lower affinity (Haiech et al., 1979; Schwaller, 2010). In contrast, crayfish SCP exists as a dimer of ~ 22 kDa subunits with 6 high-affinity calcium binding sites. Two of these sites are calcium specific while four also bind magnesium. The calcium specific sites and two of the calcium-magnesium sites demonstrate positive cooperativity, while the other two calcium-magnesium sites demonstrate negative cooperativity (Wnuk et al., 1979).

Although the precise function of SCP remains unknown, comparisons to parvalbumin offer working hypotheses. Parvalbumin probably speeds relaxation of skeletal muscles by binding free calcium concentration in the sarcoplasm following contractions (Munterner et al., 1995; Schwaller et al., 1999; Chin et al., 2003). Additionally, parvalbumin may buffer calcium levels during sustained contractions, thereby limiting increases in calcium levels that could impair muscle function. Similar roles for SCP are plausible, but no direct evidence supports such roles. Also, Hermann and Cox (1995) suggest that SCP may serve to regulate intracellular magnesium levels.

SCP cDNAs have been cloned from several invertebrates, including shrimp, *Drosophila*, and crayfish (Takagi and Konishi, 1984; Jauregui-Adell et al., 1989; Pauls et al., 1993; Kelly et al., 1997; Gao et al., 2006). *Procambarus clarkii* SCP (pcSCP1) is expressed most highly in skeletal muscle but is also found in cardiac muscle (Gao et al., 2006). Recently, we described three splice variants of crayfish SCP (pcSCP1a, pcSCP1b, and pcSCP1c) that differ in sequence across a 37 amino acid region between the second and third EF-hand domain (White et al., 2011). All three variants are highly expressed in fast-twitch muscle. The functional significance of these variants is not understood, but comparisons to parvalbumin again offer some insight.

Fish express multiple isoforms of parvalbumin, with variation across different muscle subtypes. Trout expresses at least two parvalbumin isoforms: Parv 1 and Parv 2. Red muscle of trout parr mainly expresses

* Corresponding author at: Department of Biology, 202 N. College Rd., Kenyon College, Gambier, OH 43022, United States. Tel.: +1 740 427 5399.

E-mail addresses: srohrbac@ucsd.edu (S. E. Rohrback),

Michele.Wheatly@mail.wvu.edu (M.G. Wheatly), gillenc@kenyon.edu (C.M. Gillen).

¹ Abbreviations: SCP, sarcoplasmic calcium binding protein; pcSCP, *Procambarus clarkii* sarcoplasmic calcium binding protein.

the Parv1 isoform, while the relative expression of Parv1 and Parv2 is approximately equal in white muscle of parr (Coughlin et al., 2007). Eight isoforms of parvalbumin have been identified in carp (Brownridge et al., 2009). Expression of some of these isoforms differs across a longitudinal gradient. For example, isoforms $\beta 4$ and $\beta 5$ are more prevalent in anterior axial muscle, which has faster relaxation kinetics than posterior axial muscle. Differential expression of isoforms has been observed in other fish (Schoenman et al., 2010). Additionally, functional analyses have shown that parvalbumin isoforms can display different calcium binding properties. For example, organic osmolytes have a greater influence on calcium binding by stingray PVII than on PVI (Heffron and Moerland, 2008). These studies suggest that differential expression and binding dynamics of parvalbumin isoforms may contribute to functional differences across muscles.

Manipulating the divalent cation affinities of EF-hand calcium binding proteins is an emerging therapeutic strategy (Zhang et al., 2011; Wang et al., 2013). Such work depends upon knowledge of the mechanisms that underpin divalent cation affinities. For example, recent work demonstrating that engineered troponin C can improve calcium sensitivity in diseased cardiac muscle relies upon prior work showing that conversions of hydrophobic amino acids to polar amino acids sensitize cardiac troponin C to calcium (Tikunova and Davis, 2004; Liu et al., 2012).

The crayfish SCP splice variants offer the opportunity to explore the role of SCP and to probe structure-function relationships of EF-hand calcium binding proteins. Here, we employ tryptophan fluorescence to measure conformational changes of the three splice variants in response to calcium, as alternative splicing has been shown to influence protein structure and function (Stetefeld and Ruegg, 2005; Ochoa-Leyva et al., 2013). We test that hypothesis that the splice variants have different calcium binding affinities and cooperativities.

2. Methods

2.1. Construction of expression vectors

Full length cDNAs encoding pcSCP1a (GenBank accession no. **JF692202**), pcSCP1b (GenBank accession no. **JF692203**), and pcSCP1c (GenBank accession no. **JF692204**) (White et al., 2011) were subcloned into the pET21b expression vector (Novagen, EMD Chemicals Inc., Darmstadt, Germany) using standard techniques. In brief, an NdeI restriction site was added to the 5' untranslated region of the three pcSCP1 variants in the TOPO TA cloning vector (Invitrogen, Life Technologies, Grand Island, NY). pcSCP1 open reading frames were then transferred from the TOPO TA cloning vector to the pET21b expression vector using the NdeI and XhoI restriction sites. T7 Express Competent *Escherichia coli* (New England Biolabs, Ipswich, MA) were transformed with the resultant plasmids. Each plasmid was sequenced on forward and reverse strands (Retrogen, San Diego, CA).

Expression plasmids containing pcSCP1c with targeted mutations were generated and transformed into *E. coli* (BL21(DE3)) by a commercial service (TOP Gene Technologies, Quebec, Canada). For each point mutation, an amino acid in pcSCP1c was changed to an amino acid that is conserved in pcSCP1a and pcSCP1b (White et al., 2011). Nucleotide 250, originally A, was mutated to C to generate pcSCP1c with glutamine instead of lysine at position 84 (pcSCP1c-K84Q). Nucleotides 310 and 311, originally GT, were mutated to AC to substitute tyrosine for valine at position 104 (pcSCP1c-V104Y). Both sites were mutated to generate the double mutant pcSCP1c-K84Q-V104Y.

2.2. Expression and purification of pcSCP1 proteins

Cells were grown in LB broth to OD₆₀₀ ~ 0.2 and expression was induced with IPTG. After 2 h at 37 °C with shaking at 225 rpm, cells

were collected by centrifugation, resuspended in cold Tris–HCl (20 mM, pH 7.9), sonicated (50% intensity, 3 times 10 s), and centrifuged at 13,000 g for 10 min to remove debris. To purify SCP protein from crayfish muscles, Cox et al. (1976) used gel filtration chromatography on Sephadex® G-100 columns followed by anion exchange chromatography on DEAE cellulose columns. Because pcSCP1 protein already represented a large fraction of soluble protein in induced cells, we found chromatography on 35 × 1 cm DEAE cellulose columns to be sufficient. Soluble extracts were loaded onto a column and washed for 30 min at 2 ml/min with Tris–HCl (20 mM, pH 7.9). Proteins were eluted with a high salt buffer (1 M NaCl, 20 mM Tris–HCl, pH 7.9) applied as a gradient from 0 to 100% over 280 min at 1.75 ml/min. Fractions were collected every 3.5 min and analyzed by protein assay (BCA reagent, Thermo Scientific, Brockford, IL).

Fractions containing protein were analyzed by SDS-PAGE using 12% Tris–HCl polyacrylamide gels, Laemmli sample loading buffer, and tris/glycine/SDS running buffers (Mini-PROTEAN® Tetra System, BioRad, Hercules, CA) followed by Coomassie staining. Fractions with substantial pcSCP1 (identified by molecular weight) were concentrated and had their buffer exchanged for storage buffer (200 mM MOPS, 10 μ M CaCl₂, pH 7.4) using centrifugal concentrators (30 kDa cutoff, EMD Millipore Corporation, Billerica, MA). Total protein concentration was determined by BCA assay and Coomassie stained gels were analyzed using ImageJ to determine the percent purity of pcSCP1. For each variant, all fractions with a high purity (at least 85%) of pcSCP1 were combined and diluted to 6.25 μ M. Select fractions were evaluated by native PAGE on 12% Tris–HCl polyacrylamide gels with Tris–glycine buffer systems. Some of the purified protein was stored at –20 °C in single-use aliquots for fluorescence experiments, and the remainder was stored at –70 °C.

2.3. Tryptophan fluorescence

pcSCP1 samples were diluted to 250 nM with a MOPS/EGTA buffer (200 mM MOPS; 2 mM EGTA; 0, 1, or 10 mM MgCl₂; pH 7.45; 2.5 mL final volume) in a quartz cuvette. For experiments with pcSCP1c mutants, the buffer pH was 7.15, which did not significantly alter the response of pcSCP1c wild-type protein. Fluorescence spectra were obtained using a SPEX FluoroMax-3 fluorescence spectrophotometer (Jobin Yvon, Inc, Edison, NJ) with excitation at 295 nm and emission at 303–500 nm (1 nm increments, 0.3 s/nm, 2 nm slit widths) at 21 °C. Three scans were averaged for each measurement. Fluorescence of the MOPS/EGTA buffer was measured for background subtraction. Free calcium concentrations were determined based on the pH, ionic strength, and concentration of EGTA, Ca²⁺, and Mg²⁺ using the MaxChelator program (<http://maxchelator.stanford.edu/CaMgATPEGTA-TS.htm>). To explore calcium binding, spectra were obtained in fifteen increasing concentrations of free Ca²⁺ ranging from approximately 10^{–11} to 10^{–5} M for an individual sample of pcSCP1. Spectra were taken approximately 5 min after each addition of Ca²⁺. Preliminary experiments showed no differences in integrated fluorescence values over the first 5 min after altering calcium concentration.

2.4. Analysis of fluorescence spectra

Blank-subtracted spectra were integrated and normalized based on the extreme high and low values within each experiment. To determine apparent Ca²⁺ binding affinity and cooperativity, we first applied the standard Hill model (Tables 1–3). In several instances, we were unable to obtain reasonable estimates of the Hill coefficient due to an insufficient number of data points across the calcium concentrations in the variable portion of the binding curve. Also, the standard Hill model sometimes failed to capture features of the binding curves, especially for pcSCP1c (Fig. 1) and pcSCP1b (data not shown).

Table 1
Ca²⁺ binding constants of wild-type pcSCP1 variants using standard Hill model.

Protein	0 mM Mg ²⁺	Binding constant (M)	
		1 mM Mg ²⁺	10 mM Mg ²⁺
pcSCP1a		2.8 ± 0.1 × 10 ⁻⁸	9.2 ± 0.6 × 10 ⁻⁸
pcSCP1b	2.7 ± 0.7 × 10 ⁻⁸	5.1 ± 0.3 × 10 ⁻⁸	1.2 ± 0.2 × 10 ⁻⁷
pcSCP1c	4.9 ± 0.1 × 10 ⁻⁸	1.9 ± 0.1 × 10 ⁻⁷	3.9 ± 0.1 × 10 ⁻⁷

Two-way ANOVA excluding 0 mM Mg²⁺: $F_{\text{variant}} = 369$, $F_{\text{Mg}^{2+}} = 225$, $F_{\text{interaction}} = 35$, $p_{\text{variant}} < 0.001$, $p_{\text{Mg}^{2+}} < 0.001$, $p_{\text{interaction}} < 0.001$. Two-way ANOVA excluding pcSCP1a: $F_{\text{variant}} = 119$, $F_{\text{Mg}^{2+}} = 20$, $F_{\text{interaction}} = 411$, $p_{\text{variant}} < 0.001$, $p_{\text{Mg}^{2+}} = 0.001$, $p_{\text{interaction}} < 0.001$. Values are mean ± SEM; $n = 3$ for each treatment.

To address the shortcomings of the Hill model, we also evaluated data using an equation that models two tryptophan fluorescence responses in opposite directions:

$$F = \frac{B_{\max 1}}{\left(1 + \frac{K_{d1}}{[Ca]}\right)^{\text{Hill1}}} - \frac{B_{\max 2}}{\left(1 + \frac{K_{d2}}{[Ca]}\right)^{\text{Hill2}}}$$

where F is normalized integrated fluorescence intensity and $B_{\max 1}$ and $B_{\max 2}$ are maximum changes in fluorescence intensity, K_{d1} and K_{d2} are apparent binding constants, and Hill1 and Hill2 are Hill coefficients for two separate fluorescent sites (Tables 4 and 5). We fixed $B_{\max 2}$ at 1, so that $B_{\max 1}$ represents the relative difference in maximal changes in fluorescence intensity between the two tryptophans.

Two-sample T -tests and ANOVA tests with Tukey's post-hoc comparisons were used to compare means between treatments. We were unable to estimate binding constants and Hill coefficients for pcSCP1a in 0 mM Mg²⁺ because fluorescence intensity did not plateau at the lowest calcium concentrations. Thus, we performed two separate ANOVA analyses, one excluding 0 mM Mg²⁺ data and one excluding pcSCP1a data. All statistical tests were performed using Minitab 16.2.0 (State College, PA). Values are presented as means ± SEM.

3. Results

3.1. Production and purification of pcSCP1 protein

E. coli transformed with pcSCP1 expression plasmids robustly expressed pcSCP1 protein. When these cells were induced with IPTG, pcSCP1 was the most highly expressed soluble protein based upon visual inspection of SDS-PAGE gels stained with Coomassie blue. On SDS-PAGE gels, all recombinant pcSCP1 proteins displayed a molecular mass of approximately 22 kDa, consistent with their predicted size (data not shown). Anion exchange chromatography resulted in fractions with pcSCP1 isolated to approximately 90% purity (Fig. 2).

Protein encoded by the pcSCP1 splice variants and the pcSCP1c mutants migrated with different mobility on native protein gels, consistent with their predicted pI values (Fig. 2). pcSCP1a, the variant with the highest predicted pI (4.45) migrated the slowest, while pcSCP1b (pI = 4.33) migrated the fastest. Migration of pcSCP1c (pI = 4.38) was intermediate between pcSCP1a and pcSCP1b. As expected,

Table 2
Hill coefficients for Ca²⁺ binding of wild-type pcSCP1 variants using standard Hill model.

Protein	0 mM Mg ²⁺	Hill coefficient	
		1 mM Mg ²⁺	10 mM Mg ²⁺
pcSCP1a		1.5 ± 0.0	1.5 ± 0.1
pcSCP1b	2.7 ± 0.1 ($n = 2$)	2.9 ± 0.3 ($n = 2$)	2.9 ± 1.1
pcSCP1c	2.4 ± 0.03	5.4 ± 0.1	8.3 ($n = 1$)

Two-way ANOVA excluding 0 mM Mg²⁺: $F_{\text{variant}} = 35$, $F_{\text{Mg}^{2+}} = 3.7$, $F_{\text{interaction}} = 3.1$, $p_{\text{variant}} < 0.001$, $p_{\text{Mg}^{2+}} = 0.086$, $p_{\text{interaction}} = 0.093$. Two-way ANOVA excluding pcSCP1a: $F_{\text{variant}} = 2.1$, $F_{\text{Mg}^{2+}} = 0.6$, $F_{\text{interaction}} = 0.2$, $p_{\text{variant}} = 0.170$, $p_{\text{Mg}^{2+}} = 0.439$, $p_{\text{interaction}} = 0.799$. Values are mean ± SEM; $n = 3$ for each unlabeled treatment.

Table 3
Ca²⁺ binding constants and Hill coefficient of wild-type and mutant pcSCP1 in 1 mM Mg²⁺ using standard Hill model.

Protein	Binding constant (M)	Hill coefficient
pcSCP1c-WT	2.5 ± 0.2 × 10 ⁻⁷ ^a	4.5 ± 0.2
pcSCP1c-K84Q	2.0 ± 0.1 × 10 ⁻⁷ ^b	4.3 ± 1.0
pcSCP1c-V104Y	1.9 ± 0.1 × 10 ⁻⁷ ^b	4.9 ± 0.5
pcSCP1c-K84Q-V104Y	1.7 ± 0.1 × 10 ⁻⁷ ^b	3.8 ± 0.5

Means that do not share a letter are statistically different at $p < 0.05$ (ANOVA with Tukey's comparisons). Values are mean ± SEM; $n = 3$ for each treatment.

substituting a polar glutamine for a basic lysine increased electrophoretic mobility of the pcSCP1c-K84Q mutant, shifting it towards pcSCP1b. Substituting tyrosine for valine did not substantially affect mobility of the pcSCP1c-V104Y mutant.

3.2. Tryptophan fluorescence

Upon excitation at 295 nm, recombinant pcSCP1c variants and mutants fluoresced with a peak emission between 345 and 350 nm, consistent with tryptophan fluorescence (Fig. 3a). Fluorescent spectra were strongly influenced by free calcium concentration (Fig. 3b). Integrated fluorescence intensity of pcSCP1a decreased with increasing calcium concentration. In contrast, fluorescence intensity of pcSCP1b and pcSCP1c increased with increasing calcium. The magnitude of the fluorescence response to calcium was greater in pcSCP1a than in pcSCP1b and pcSCP1c. Fluorescence intensity decreased approximately 30% from the highest to lowest free calcium levels in pcSCP1a, while it increased less than 15% in pcSCP1b and pcSCP1c. Additionally, increasing calcium shifted the emission peak of pcSCP1a from 349 nm at the lowest calcium concentrations to 345 nm at the highest calcium concentrations. In contrast, emission spectra of pcSCP1b and pcSCP1c peaked at approximately 345 nm across all calcium concentrations.

3.3. Comparison of calcium binding curve models

We first evaluated calcium binding curves using a standard Hill equation. While the standard Hill equation accurately modeled pcSCP1a in 1 and 10 mM Mg²⁺, it typically failed to capture the full shape of pcSCP1b and pcSCP1c binding curves, especially at the highest and lowest calcium concentrations. Because there are two tryptophans in pcSCP1 and the fluorescence response of pcSCP1a was in the opposite direction of pcSCP1b and pcSCP1c, we also fitted calcium binding curves

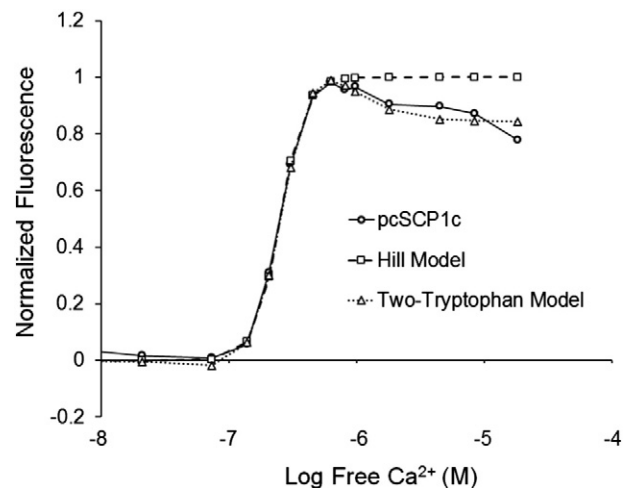
**Fig. 1.** Comparison of data from a representative calcium binding experiment (wild-type pcSCP1c; circles, solid line) to curves fit using a standard Hill model (squares, dashed line) and a model with two tryptophans responding in opposite directions to calcium (triangles, dotted line). Values below 10⁻⁸ M free Ca²⁺ are not depicted.

Table 4
Ca²⁺ binding constants (*K*_d1) and Hill coefficients (Hill1) for pcSCP1 variants using two tryptophan model.

Protein	Binding constant (M)		Hill coefficient	
	1 mM Mg ²⁺	10 mM Mg ²⁺	1 mM Mg ²⁺	10 mM Mg ²⁺
pcSCP1b	6.4 ± 0.8 × 10 ^{−8a}	2.0 ± 0.3 × 10 ^{−7a}	2.2 ± 0.3 ^a	2.2 ± 0.5 ^a
pcSCP1c	2.0 ± 0.1 × 10 ^{−7b}	5.6 ± 0.1 × 10 ^{−7b}	3.0 ± 0.1 ^a	3.3 ± 0.1 ^a

Means for pcSCP1b and pcSCP1c were compared for each parameter by two-sample *T*-test. Means that do not share a letter are statistically different at *p* < 0.05. Values are mean ± SEM; *n* = 3 for each treatment.

using an equation that models two independent tryptophans that fluoresce in response to calcium. This equation more effectively fit the shape of pcSCP1c (Fig. 1) and pcSCP1b (data not shown) than the standard Hill equation, but did not effectively describe the pcSCP1a curves (not shown). Though the two tryptophan model more accurately describes the binding curves of pcSCP1b and pcSCP1c, both models return similar binding constants and point to the same conclusions. Neither model effectively captures the gradual decrease in fluorescence that occurs between 10^{−11} M and approximately 10^{−8} M Ca²⁺ (e.g. Fig. 4), particularly in the absence of Mg²⁺. However, the lowest Ca²⁺ concentrations do not represent physiologically relevant conditions. Also, parvalbumin becomes an intrinsically disordered protein in the absence of divalent metals (Permyakov et al., 2008), and pcSCP1 may also lack ordered tertiary structure at very low Ca²⁺ levels. Thus, fluorescence changes at the lowest Ca²⁺ concentrations may not represent authentic Ca²⁺ binding events.

3.4. Standard Hill model

When the standard Hill model was applied, apparent steady-state calcium binding affinity (*K*_d) of pcSCP1 variants ranged from 2.7 ± 0.7 × 10^{−8} M to 3.9 ± 0.1 × 10^{−7} M (Table 1). Increasing Mg²⁺ concentration increased the *K*_d for calcium of all three pcSCP1 variants (Fig. 4). Because we were unable to estimate binding constants for pcSCP1a in 0 mM Mg²⁺ due to the shape of the binding curves, we statistically evaluated the effect of Mg²⁺ concentration on pcSCP1b and pcSCP1c separately from pcSCP1a. For both pcSCP1b and pcSCP1c, *K*_d for calcium binding increased significantly with increasing magnesium concentrations, varying by nearly an order of magnitude (Table 1). Calcium binding affinity of pcSCP1a was more than 3-fold greater in 1 mM Mg²⁺ compared to 10 mM Mg²⁺ (Table 1; two-sample *t*-test, *p* = 0.009).

The three pcSCP1c variants displayed different calcium binding constants (Fig. 4, ANOVA, *p* < 0.001). pcSCP1a consistently displayed the lowest *K*_d, whereas pcSCP1c had the highest *K*_d at each Mg²⁺ concentration (Table 1). In 1 mM Mg²⁺, *K*_d of pcSCP1b was approximately 80% greater than that of pcSCP1a, though this difference was not statistically significant (Tukey's test, *p* > 0.05). *K*_d of pcSCP1c was more than 250% greater than that of pcSCP1b in 1 mM Mg²⁺ (Tukey's test, *p* < 0.05). Hill coefficients significantly differed among the splice variants (Table 2, ANOVA, *p* < 0.001). Hill coefficients were well above 1 for pcSCP1b and pcSCP1c, suggesting cooperative binding of calcium. At 1 mM Mg²⁺, the Hill coefficient of pcSCP1c was above 5, while it was approximately 3 for pcSCP1b. Hill coefficients for pcSCP1a were consistently lower, averaging about 1.5.

Table 5
Ca²⁺ binding constants (*K*_d1) and Hill coefficients (Hill1) of pcSCP1c mutants in 1 mM - Mg²⁺ using two tryptophan model.

	Binding constant	Hill coefficients
pcSCP1c-WT	2.7 ± 0.2 × 10 ^{−7} M ^a	3.2 ± 0.1 ^a
pcSCP1c-K84Q	2.1 ± 0.1 × 10 ^{−7} M ^b	3.1 ± 0.3 ^a
pcSCP1c-V104Y	2.0 ± 0.1 × 10 ^{−7} M ^b	3.3 ± 0.2 ^a
pcSCP1c-K84Q-V104Y	1.9 ± 0.1 × 10 ^{−7} M ^b	2.7 ± 0.2 ^a

Means that do not share a letter are statistically different at *p* < 0.05 (ANOVA with Tukey's comparisons). Values are mean ± SEM; *n* = 3 for each treatment.

Apparent calcium binding affinity of pcSCP1c was increased by mutations that converted one or two amino acids of the variable region to the amino acid found in pcSCP1a and pcSCP1b (Fig. 5). The pcSCP1c to pcSCP1a/b mutants had 20–32% lower *K*_d for calcium binding compared to wild-type pcSCP1c (Table 3). The double mutant had the largest increase in affinity, though no significant differences in *K*_d were detected among the mutants. The Hill coefficients for mutants of pcSCP1c did not significantly differ from wild-type pcSCP1c (Table 3).

3.5. Two-tryptophan model

The two-tryptophan model analysis models fluorescence changes at two tryptophans, arbitrarily labeled tryptophan 1 and tryptophan 2. Fluorescence at tryptophan 1 increases in response to increasing calcium while fluorescence decreases at tryptophan 2. Measured tryptophan fluorescence of both pcSCP1b and pcSCP1c increases in response to increased calcium. Thus, for these variants we expected the magnitude of fluorescence changes at tryptophan 1 (*B*_{max}1) to exceed those at tryptophan 2 (*B*_{max}2). Indeed, *B*_{max}1 was 1.84 ± 0.03 (*n* = 12) fold greater than *B*_{max}2, with no difference between pcSCP1b and pcSCP1c and no differences between 1 and 10 mM Mg²⁺. Similarly, *B*_{max}1 was 1.73 ± 0.02 (*n* = 9) fold greater than *B*_{max}2 for the pcSCP1c mutants, with no significant differences among the mutants or between the mutants and pcSCP1c controls. Thus, the maximal increase in fluorescence at tryptophan 1 was greater than the maximal decrease at tryptophan 2 by approximately the same amount for pcSCP1b and pcSCP1c across all conditions.

No differences were detected in binding constants or Hill coefficients between pcSCP1b and pcSCP1c at tryptophan 2. For pcSCP1b and pcSCP1c, the average calcium binding constant for tryptophan 2 was 2.5 ± 0.5 × 10^{−7} M in 1 mM Mg²⁺ and 6.2 ± 1.0 × 10^{−7} M in 10 mM Mg²⁺. Hill coefficients at tryptophan 2 were 1.5 ± 0.1 in 1 mM Mg²⁺ and 2.3 ± 0.2 in 10 mM Mg²⁺. For the pcSCP1c mutants, the calcium binding constant for tryptophan 2 was 3.5 ± 0.5 × 10^{−7} M

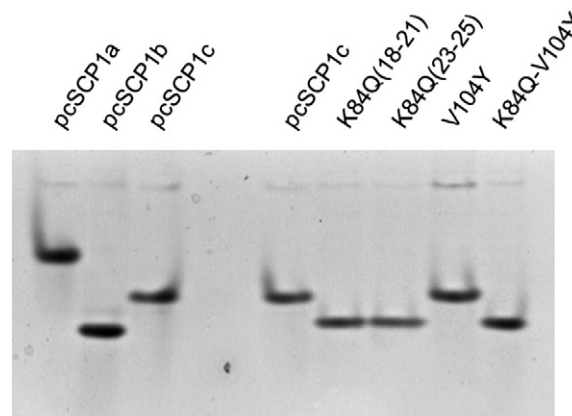


Fig. 2. Native protein gel electrophoresis of pcSCP1 variants expressed in *E. coli* and purified by DEAE chromatography. First three lanes are wild-type proteins; last five lanes are wild-type pcSCP1c and pcSCP1c point mutations. See Methods for explanation of the mutations. Two sets of pooled fractions (18–21 and 23–25) from DEAE chromatography are shown for the K84Q mutation.

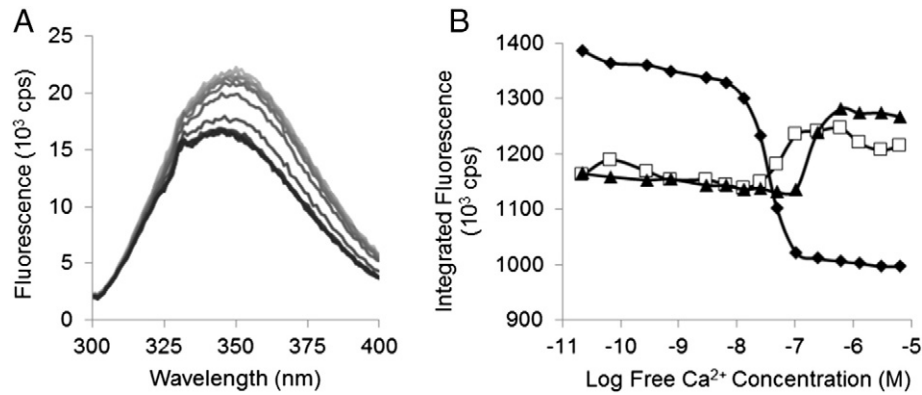


Fig. 3. Panel A. Exemplary set of blank-subtracted fluorescence spectra for pcSCP1a in 1 mM Mg^{2+} across a range of free Ca^{2+} concentrations ranging from 8.4×10^{-12} to 3.1×10^{-5} . Traces are shaded according to Ca^{2+} concentration, with darkest lines representing the highest concentrations. Panel B. Relationship between integrated fluorescence intensity and free Ca^{2+} concentration from a single representative experiment using pcSCP1a (filled diamonds), pcSCP1b (open squares), and pcSCP1c (closed triangles) in 1 mM Mg^{2+} .

and Hill coefficient was 1.6 ± 0.1 , again with no differences among the mutants or between the mutants and pcSCP1c controls. Evidently, tryptophan 2 detects fluorescence changes in response to Ca^{2+} that are the same between pcSCP1b and pcSCP1c.

At tryptophan 1, calcium binding constants mirrored the output of the standard Hill model. Calcium binding constants were significantly lower for pcSCP1b than pcSCP1c in both 1 and 10 mM Mg^{2+} (Table 4), and the values were approximately the same as those from the standard model. Similarly, calcium binding constants detected at

tryptophan 1 of all three pcSCP1c mutants were lower than control pcSCP1c (Table 5). Again, binding constants were approximately the same as those from the standard model. On the other hand, the Hill coefficient for pcSCP1b was approximately 2, while that of pcSCP1c was approximately 3 (Tables 4 and 5), both lower than the corresponding values from the standard model (Tables 2 and 3).

4. Discussion

The structural basis of divalent cation affinities of EF-hand proteins is incompletely understood. Here, we take advantage of a natural experiment—three splice variants of crayfish SCP—to explore structure–function in an EF-hand calcium buffering protein. We hypothesized that the pcSCP splice variants differ in their calcium binding properties. Two results reported here support this hypothesis. First, structural changes in response to calcium varied among wild-type pcSCP1a, pcSCP1b, and pcSCP1c. Second, amino acid substitutions confirmed that specific residues in the variable region of pcSCP1 contribute to differences between pcSCP1b and pcSCP1c.

4.1. Properties of recombinant pcSCP1

The properties of our purified recombinant SCP are consistent with those obtained by others of SCP purified from crayfish muscle. The three pcSCP1 variants migrated differently on non-denaturing gels, in accordance with their divergent amino acid sequences. Similarly, SCP isolated from crayfish muscle migrates in three distinct bands on non-denaturing gels (Chen et al., 2013). Combined, these findings indicate

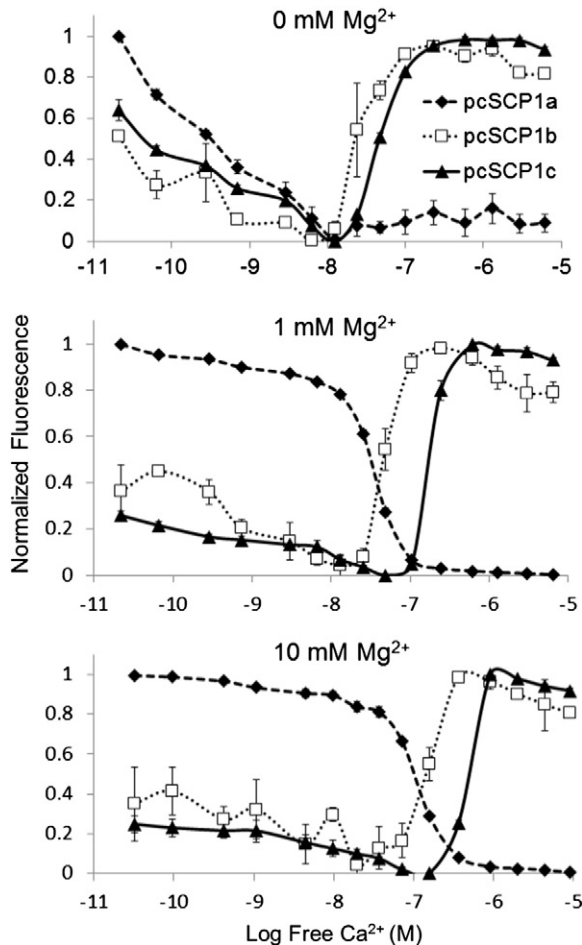


Fig. 4. Relationships between free Ca^{2+} concentration and normalized fluorescence of wild-type pcSCP1a (filled diamonds), pcSCP1b (open squares), and pcSCP1c (closed triangles) in 0 mM Mg^{2+} (top), 1 mM Mg^{2+} (middle), 10 mM Mg^{2+} (bottom). Symbols represent mean \pm SEM; $n = 3$ for each treatment.

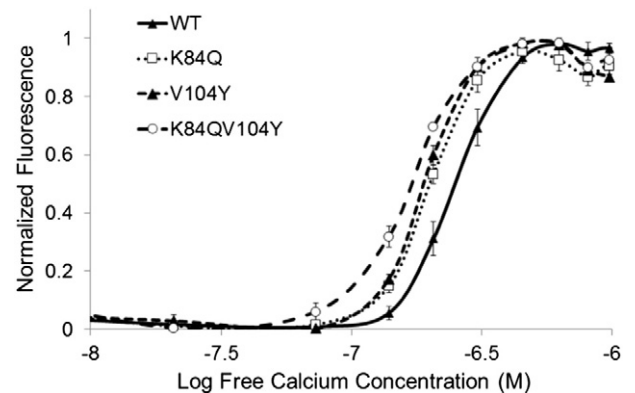


Fig. 5. Relationship between free Ca^{2+} concentration and normalized fluorescence of wild-type pcSCP1c (filled diamonds), pcSCP1c-K84Q (open squares), pcSCP1c-V104Y (closed triangles), and pcSCP1c-K84Q-V104Y (open circles) in 1 mM Mg^{2+} . Values below 10^{-8} M free calcium are not shown. Symbols represent mean \pm SEM; $n = 3$ for each treatment.

that all three splice variants are expressed in crayfish muscle, consistent with our analysis of mRNA transcripts in previous work (White et al., 2011).

4.2. Differential fluorescence responses of pcSCP1 to calcium

The most conspicuous difference between the pcSCP1 splice variants was the opposite fluorescent response of pcSCP1a compared to pcSCP1b and pcSCP1c. Tryptophan fluorescence of the pcSCP1a protein increased as calcium decreased, whereas fluorescence of pcSCP1b and pcSCP1c decreased. Prior work supports such opposing responses to calcium. Cox and Stein (1981) observed an increase in tryptophan fluorescence with decreased calcium during the transition from calcium-saturated to magnesium-saturated SCP isolated from the sandworm *Nereis* (Cox and Stein, 1981). In contrast, Wnuk et al. (1981) studied the tryptophan fluorescence responses of SCP purified from crayfish muscle (Wnuk et al., 1981) and found that fluorescence decreased with the transition from calcium-saturated to magnesium-saturated SCP. This finding is consistent with their measurement of pcSCP1a (called SCPI by Wnuk et al.) as the most abundant SCP in crayfish muscle (Wnuk and Jauregui-Adell, 1983) and our measurement of decreased fluorescence in response to calcium of that variant.

The proteins encoded by the pcSCP1 variants each contain two tryptophans, both outside the variable region. The opposite tryptophan fluorescence responses of pcSCP1 variants suggest that fluorescence at the two tryptophans may respond in opposite directions to changes in calcium. This scenario is plausible because the two tryptophans in pcSCP1 are probably located far apart in the protein's tertiary structure. When pcSCP1 tryptophans (residues 5 and 62) are mapped onto the tertiary structure of the *Nereis diversicolor* SCP (Vijay-Kumar and Cook, 1992), the tryptophans reside on opposite sides of the protein. Our data suggest that the changes in fluorescence in one of the two tryptophans are masked in pcSCP1a, while two tryptophans contribute to the fluorescence response of pcSCP1b and pcSCP1c.

Our results support the above interpretation. First, the calcium binding curves of pcSCP1a showed simple sigmoidal binding profiles, suggesting involvement of only a single tryptophan. Moreover, the standard Hill equation modeled the pcSCP1a curves well. In contrast, pcSCP1b and pcSCP1c calcium binding curves displayed unusual profiles, including a gradual decrease in fluorescence intensity following the sharp rise in response to increased calcium. These curves were better described by the two tryptophan model than the standard Hill equation. Also, the standard Hill equation returned unreasonably high Hill coefficients for pcSCP1c. Hill coefficients above five are unlikely because there are only six calcium binding site per SCP dimer and two display negative cooperativity (Wnuk et al., 1979). In contrast, the two tryptophan equation returned Hill coefficients for pcSCP1c of about three, a reasonable value.

While our data support the two-tryptophan model, they do not exclude the possibility that only one tryptophan contributes to the observed fluorescence changes. For example, non-specific binding could contribute to some of the drift in fluorescence at high and low Ca^{2+} concentrations. Moreover, our models do not allow us to assign binding to specific sites on the pcSCP dimer. It is possible that tryptophan fluorescence only captures binding to some subset of the 6 binding sites per dimer, and our data may reflect combined fluorescence changes resulting from binding at multiple sites. Further experiments will be necessary to conclusively differentiate between the one and two tryptophan models. However, our main conclusions are not dependent upon our choice of model. Both models return quantitatively similar apparent calcium binding affinities, and these affinities differ among the pcSCP1 variants regardless of which model we employ.

If fluorescence responses of pcSCP1a reflect responses of different tryptophans, then comparisons of binding affinities between pcSCP1a and the other variants must be made with caution. Indeed, we estimated lower Hill coefficients for pcSCP1a than pcSCP1b or pcSCP1c, suggesting

that different calcium binding sites might be monitored by the two tryptophans. However, analysis by both the standard Hill model and the two tryptophan model supports the conclusion that pcSCP1a has substantially higher calcium affinity than pcSCP1c. Because fluorescence of pcSCP1a decreased in response to calcium, its response is mediated by tryptophan 2 in our two tryptophan model. In the two tryptophan model, the calcium binding constant for tryptophan 2 of pcSCP1c was about 2.5×10^{-7} , approximately an order of magnitude greater than the binding constant for pcSCP1a. Calcium binding constants of pcSCP1b and pcSCP1c obtained from the standard Hill equation were also higher than that of pcSCP1a.

Comparisons between pcSCP1b and pcSCP1c are more reliable than comparisons that include pcSCP1a because fluorescence of pcSCP1b and pcSCP1c respond similarly to calcium. Moreover, according to the two site model, the relative contributions of the two tryptophan sites are the same for pcSCP1b and pcSCP1c.

4.3. Calcium binding constants

The calcium binding constants reported in this paper range from 2.7×10^{-8} to 5.6×10^{-7} M and are consistent with previous studies of crayfish SCP. Prior work indicates that changes in tryptophan fluorescence in response to calcium mainly represent binding to the calcium-specific sites on crayfish SCP (Wnuk et al., 1981). The calcium binding constants for these sites were approximately 5×10^{-8} for SCP purified from crayfish muscle, which is heavily enriched in pcSCP1a (called SCPI by Wnuk and Jauregui-Adell, 1983). Homodimers of the protein encoded by pcSCP1b (called SCPIII by Wnuk and Jauregui-Adell, 1983) display a slightly lower calcium affinity, with a binding constant of approximately 1×10^{-7} assessed in 1 mM Mg^{2+} (Wnuk and Jauregui-Adell, 1983). In our experiments, pcSCP1b also displayed lower apparent calcium binding affinity than pcSCP1a.

The apparent calcium binding affinity of pcSCP1b was substantially greater than pcSCP1c in 1 and 10 mM Mg^{2+} . This approximately two-fold shift in apparent calcium binding affinity must result from the 13 amino acid differences between pcSCP1b and pcSCP1c in the 37 amino acid variable region, which lies almost entirely between the 2nd and 3rd EF-hand calcium-binding domains (White et al., 2011). Influences on calcium binding by substitutions outside the calcium binding domains are plausible. For example, work on troponin C demonstrates that amino acid substitutions outside the immediate calcium chelating domain can alter calcium affinity (Tikunova et al., 2002).

The site-directed mutagenesis studies offer the most convincing evidence that differences in the variable region of pcSCP1 influence calcium binding affinity. We mutated amino acids in the variable region of pcSCP1c to match amino acids that are conserved in both pcSCP1a and pcSCP1b. Because both pcSCP1a and pcSCP1b have higher apparent calcium affinity than wild-type pcSCP1c, we predicted that these mutations would increase the affinity of pcSCP1c. Indeed, both single and double mutations of pcSCP1c shifted the calcium binding constants lower. However, even the double mutation shifted affinity only by about 30%, whereas wild-type pcSCP1b had a calcium binding constant more than 67% lower than pcSCP1c. Thus other amino acids in the variable region also contribute to differences in calcium binding affinity between pcSCP1b and pcSCP1c and deserve further investigation.

4.4. Summary

This work demonstrates that the three splice variants of pcSCP1 differ in their calcium binding properties. The implications of these differences for crayfish muscle function are unknown. However, one possibility is that by expressing SCP splice variants with a range of calcium binding affinities, crayfish muscle is able to buffer calcium across a broader range of concentrations than would otherwise be possible. Two amino acids in the variable region—lysine at position 84 and valine at position 104 of pcSCP1c—contribute to differences among the

splice variants. Interpretation of our data was complicated by the presence of two tryptophans in the pcSCP1 sequence. Future studies in which one of the two tryptophans is mutated would test the validity of the two tryptophan model. Moreover, further mutation of residues in the variable region is needed to fully explain the structural basis of differences between the pcSCP1 variants.

Acknowledgments

We thank Drs. Jonathan Davis, Yongping Gao, Harry Gill, Bradley Hartlaub, John Hofferberth, James Keller, Andrew Kerkhoff, and Robert Mauck for technical assistance and helpful discussion. We also appreciate the insightful comments of two anonymous reviewers. This research was partly supported by the National Science Foundation grant IBN 0445202 and by the Kenyon College Summer Science Scholars program.

References

- Brownridge, P., de Mello, L.V., Peters, M., McLean, L., Claydon, A., Cossins, A.R., Whitfield, P.D., Young, I.S., 2009. Regional variation in parvalbumin isoform expression correlates with muscle performance in common carp (*Cyprinus carpio*). *J. Exp. Biol.* 212, 184–193.
- Chen, H.L., Cao, M.J., Cai, Q.F., Su, W.J., Mao, H.Y., Liu, G.M., 2013. Purification and characterisation of sarcoplasmic calcium-binding protein, a novel allergen of red swamp crayfish (*Procambarus clarkii*). *Food Chem.* 139, 213–223.
- Chin, E.R., Grange, R.W., Viau, F., Simard, A.R., Humphries, C., Shelton, J., Bassel-Duby, R., Williams, R.S., Michel, R.N., 2003. Alterations in slow-twitch muscle phenotype in transgenic mice overexpressing the Ca^{2+} buffering protein parvalbumin. *J. Physiol.* 547, 649–663.
- Coughlin, D.J., Solomon, S., Wilwert, J.L., 2007. Parvalbumin expression in trout swimming muscle correlates with relaxation rate. *Comp. Biochem. Physiol. A* 147, 1074–1082.
- Cox, J.A., Stein, E.A., 1981. Characterization of a new sarcoplasmic calcium-binding protein with magnesium-induced cooperativity in the binding of calcium. *Biochemistry* 20, 5430–5436.
- Cox, J.A., Wnuk, W., Stein, E.A., 1976. Isolation and properties of a sarcoplasmic calcium binding proteins from crayfish. *Biochemistry* 15, 2613–2618.
- Gao, Y., Gillen, C.M., Wheatly, M.G., 2006. Molecular characterization of the sarcoplasmic calcium-binding protein (SCP) from crayfish *Procambarus clarkii*. *Comp. Biochem. Physiol. B* 144, 478–487.
- Haiech, J., Derancourt, J., Pechere, J.F., Demaille, J.G., 1979. Magnesium and calcium binding to parvalbumins: evidence for differences between parvalbumins and an explanation of their relaxing function. *Biochemistry* 18, 2752–2758.
- Heffron, J.K., Moerland, T.S., 2008. Parvalbumin characterization from the euryhaline stingray *Dasyatis sabina*. *Comp. Biochem. Physiol. A* 150, 339–346.
- Heizmann, C.W., Berchtold, M.W., Rowleron, A.M., 1982. Correlation of parvalbumin concentration with relaxation speed in mammalian muscles. *Proc. Natl. Acad. Sci. U. S. A.* 79, 7243–7247.
- Hermann, A., Cox, J.A., 1995. Sarcoplasmic calcium-binding protein. *Comp. Biochem. Physiol. B* 111, 337–345.
- Jauregui-Adell, J., Wnuk, W., Cox, J.A., 1989. Complete amino acid sequence of the sarcoplasmic calcium-binding protein SCP-I from crayfish *Astacus leptodactylus*. *FEBS J.* 243, 209–212.
- Kelly, L.E., Phillips, A.M., Delbridge, M., Stewart, R., 1997. Identification of a gene family from *Drosophila melanogaster* encoding proteins with homology to invertebrate sarcoplasmic calcium-binding proteins (SCPs). *Insect Biochem. Mol. Biol.* 27, 783–792.
- Leberer, E., Pette, D., 1986a. Immunochemical quantification of sarcoplasmic reticulum Ca-ATPase, of calsequestrin and of parvalbumin in rabbit skeletal muscles of defined fiber composition. *Eur. J. Biochem.* 156, 489–496.
- Leberer, E., Pette, D., 1986b. Neural regulation of parvalbumin expression in mammalian skeletal muscle. *Biochem. J.* 235, 67–73.
- Liu, B., Lee, R.S., Biesiadecki, B.J., Tikunova, S.B., Davis, J.P., 2012. Engineered troponin C constructs correct disease-related cardiac myofilament calcium sensitivity. *J. Biol. Chem.* 287, 20027–20036.
- Muntener, M., Kaser, L., Weber, J., Berchtold, M.W., 1995. Increase of skeletal muscle relaxation speed by direct injection of parvalbumin cDNA. *Proc. Natl. Acad. Sci. U. S. A.* 92, 6504–6508.
- Ochoa-Leyva, A., Montero-Morán, G., Saab-Rincón, G., Briebe, L.G., Soberón, X., 2013. Alternative splice variants in TIM barrel proteins from human genome correlate with the structural and evolutionary modularity of this versatile protein fold. *PLoS ONE* 8, e70582.
- Pauls, T.L., Cox, J.A., Heizmann, C.W., Hermann, A., 1993. Sarcoplasmic calcium-binding protein in *Aplysia* nerve and muscle cells. *Eur. J. Neurosci.* 5, 549–559.
- Permyakov, S.E., Bakunts, A.G., Denesnyuk, A.I., Knyazeva, E.L., Uversky, V.N., Permyakov, E.A., 2008. Apo-parvalbumin as an intrinsically disordered protein. *Proteins: Struct., Funct., Bioinf.* 72, 822–836.
- Schoenman, E.R., Chiaro, J.A., Jones, A., Bastin, L.D., Coughlin, D.J., 2010. A comparative analysis of parvalbumin expression in pinfish (*Lagodon rhomboides*) and toadfish (*Opsanus* sp.). *Comp. Biochem. Physiol. A* 155, 91–99.
- Schwaller, B., 2010. Cytosolic Ca^{2+} buffers. *Cold Spring Harbor Perspectives in Biology* 2 (Article No.: a004051).
- Schwaller, B., Dick, J., Dhoot, G., Carroll, S., Vrbova, G., Nicotera, P., Pette, D., Wyss, A., Bluetmann, H., Hunziker, W., Celio, M.R., 1999. Prolonged contraction-relaxation cycle of fast-twitch muscles in parvalbumin knockout mice. *Am. J. Physiol. Cell Physiol.* 276, C395–C403.
- Stetefeld, J., Ruegg, M.A., 2005. Structural and functional diversity generated by alternative mRNA splicing. *Trends Biochem. Sci.* 30, 515–521.
- Takagi, T., Konishi, K., 1984. Amino-acid sequence of the beta chain of sarcoplasmic calcium binding protein obtained from shrimp tail muscle. *J. Biochem. (Tokyo)* 96, 59–68.
- Tikunova, S.B., Davis, J.P., 2004. Designing calcium-sensitizing mutations in the regulatory domain of cardiac troponin C. *J. Biol. Chem.* 279, 35341–35352.
- Tikunova, S.B., Rall, J.A., Davis, J.P., 2002. Effect of hydrophobic residue substitutions with glutamine on Ca^{2+} binding and exchange with the N-domain of troponin C†. *Biochemistry* 41, 6697–6705.
- Vijay-Kumar, S., Cook, W.J., 1992. Structure of a sarcoplasmic calcium-binding protein from *Nereis diversicolor* refined at 2 · 0 Å resolution. *J. Mol. Biol.* 224, 413–426.
- Wang, W., Barnabei, M.S., Asp, M.L., Heinis, F.I., Arden, E., Davis, J., Braunlin, E., Li, Q., Davis, J.P., Potter, J.D., Metzger, J.M., 2013. Noncanonical EF-hand motif strategically delays Ca^{2+} buffering to enhance cardiac performance. *Nat. Med.* 19, 305–312.
- White, A.J., Northcutt, M.J., Rohrback, S.E., Carpenter, R.O., Niehaus-Sauter, M.M., Gao, Y., Wheatly, M.G., Gillen, C.M., 2011. Characterization of sarcoplasmic calcium binding protein (SCP) variants from freshwater crayfish *Procambarus clarkii*. *Comp. Biochem. Physiol. B* 160, 8–14.
- Wnuk, W., Jauregui-Adell, J., 1983. Polymorphism in high affinity calcium binding proteins from crustacean sarcoplasm. *Eur. J. Biochem.* 131, 177–182.
- Wnuk, W., Cox, J.A., Kohler, L.G., Stein, E.A., 1979. Calcium binding and magnesium binding properties of a high affinity calcium binding protein from crayfish sarcoplasm. *J. Biol. Chem.* 254, 5284–5289.
- Wnuk, W., Cox, J.A., Stein, E.A., 1981. Structural changes induced by calcium and magnesium in a high affinity calcium binding protein from crayfish sarcoplasm. *J. Biol. Chem.* 256, 11538–11544.
- Zhang, J., Shettigar, V., Zhang, G.C., Kindell, D.G., Liu, X., Lopez, J.J., Yerrimuni, V., Davis, G.A., Davis, J.P., 2011. Engineering parvalbumin for the heart: optimizing the Mg^{2+} binding properties of rat R-parvalbumin. *Front. Physiol.* 2, 77.